Surface Crystallization in a Liquid AuSi Alloy.

Oleg G. Shpyrko[1,2*], Reinhard Streitel[1],
Venkatachalapathy S. K. Balagurusamy[1], Alexei Y. Grigoriev[1],
Moshe Deutsch[3], Benjamin M. Ocko[4], Mati Meron[5],
Binhua Lin[5], Peter S. Pershan[1]

[1]Department of Physics and Division of Engineering and Applied Sciences,
Harvard University, Cambridge, MA 02138, USA
[2]Center for Nanoscale Materials, Argonne National Laboratory, Argonne, IL 60439, USA
[3]Department of Physics, Bar-Ilan University, Ramat-Gan 52900, Israel
[4]Condensed Matter Physics and Materials Science Department,
Brookhaven National Laboratory, Upton NY 11973, USA
[5]Center for Advanced Radiation Sources, University of Chicago, Chicago, IL 60637, USA
*To whom correspondence should be addressed. E-mail: oshpyrko@anl.gov.
4 April 2006; accepted 25 May 2006; doi:10.1126/science.1128314

X-ray measurements reveal a crystalline monolayer at the surface of the eutectic liquid $Au_{82}Si_{18}$, at temperatures above the alloy's melting point. Surface-induced atomic layering, the hallmark of liquid metals, is also found below the crystalline monolayer. The layering depth, however, is threefold greater than that of all liquid metals studied to date. The crystallinity of the surface monolayer is notable, considering that AuSi does not form stable bulk crystalline phases at any concentration and temperature and that no crystalline surface phase has been detected thus far in any pure liquid metal or nondilute alloy. These results are discussed in relation to recently suggested models of amorphous alloys.

Surface melting - the coexistence of a liquid surface layer with the bulk crystal at temperatures below the bulk melting point T_m - has been observed in a wide range of materials (*1,2*) and occurs because the entropy of molecules at the free surface is greater than that in the bulk due to the reduced number of their near-neighbors. The opposite effect, surface freezing, where a crystalline surface layer coexists with its molten bulk, is much rarer. Surface freezing has been observed, however, in complex liquids composed of high-anisotropy molecules, such as molten unary or binary alkanes and their derivatives (*3*), and in liquid crystals (*4*). Theory assigns the occurrence of this effect to the highly anisotropic shape of the molecules and to their lengths being greater than the interfacial width (*5*).

Freezing of the surface-segregated component into a two-dimensional (2D) solid layer has also been reported recently in the very dilute binary metallic alloys $Ga_{99.948}Pb_{0.052}$ (*6*) and $Ga_{99.986}Tl_{0.014}$ (*7*). A different ordering effect, surface-induced layering consisting of stratified layers (Fig. 1) near the vapor interface (*8,9*), has been observed in all liquid metals and alloys studied to date. The decay of the layering order with depth is exponential and has a range equal to the bulk liquid correlation length (two to three atomic diameters). No surface-parallel ordering was found within these layers in any elemental liquid metal. Similar layering, along with epitaxially induced surface-parallel order, has also been observed in both metallic and nonmetallic liquids near solid/liquid interfaces (*10,11,12*).

We present evidence for surface crystallization and enhanced surface layering in the liquid $Au_{82}Si_{18}$ eutectic alloy of a type unlike that previously reported for any liquid metal or alloy. A surface monolayer that exhibits lateral long-range crystalline order was found above the eutectic temperature T_e =359 °C. Beneath this monolayer, seven to eight layers occur that are liquid in the lateral direction but well defined in the normal direction. The crystalline surface monolayer and the enhancement of the surface-induced layering range beyond the two to three layers observed in all other liquid metals studied to date clearly have a common origin. The

surface-frozen monolayer undergoes a first-order transition into a different surface phase 12 °C above T_e.

These unusual surface structures probably result from the equally unusual bonding properties of metastable amorphous bulk AuSi. AuSi, the first metallic alloy found to exhibit a glassy solid phase (*13*), remains one of the most puzzling amorphous solids. Silicon-rich amorphous AuSi is a semiconductor, has a low packing density, and has a low atomic coordination number (4 to 5). Its main structural motif is a continuous random network of covalently bonded Si atoms. The Au-rich alloy, however, is a metallic glass, almost as dense as a face-centered cubic lattice, has a high atomic coordination number (8 to 9), and has a random hard-sphere packing (*14*). Such random packing in amorphous metals was recently shown to consist of interpenetrating clusters, the outer atoms of which are shared by adjacent clusters (*15,16*). Because Si has a lower surface tension than Au, the surface of liquid AuSi alloy is Si-rich, so atomic packing and bonding at the surface might be expected to be more like that of the covalently bonded Si-rich alloys than the metallic Au-rich bulk.

The existence of a very deep eutectic (for $Au_{82}Si_{18}$) at $T_e \approx$359 °C, much below T_m =1063 °C of Au and T_m =1412 °C of Si (Fig. 2A, inset), arises from the bonding effects discussed above. Below T_e, AuSi phase-separates in thermodynamic equilibrium into crystalline Au and Si, with no mutual solid solubility and no stable crystalline intermetallic compounds, whereas metastable amorphous AuSi phases can be achieved by rapid quenching, sputtering and other techniques (*14*).

X-ray reflectivity off a liquid surface, $R(q_z)$, is measured as a function of the grazing angle of incidence α. Here $q_z = (4\pi/\lambda)\sin\alpha$ is the surface-normal wavevector transfer and λ is the x-rays' wavelength. The ratio R/R_F, where R_F is the theoretical reflectivity off of an ideally flat and abrupt liquid-vapor interface, depends on the surface-normal electron density profile $\rho(z)$. A layered interface produces a Bragg-like peak in $R(q_z)/R_F(q_z)$ because of the constructive

interference of the rays reflected from the periodically ordered surface layers (*8*). The larger the number of layers, the higher is the layering peak. Fig. 2A demonstrates that the AuSi layering peak at 370 °C is at least one order of magnitude higher than for the standard layering profile observed in all elemental liquids measured to date (*17*). This result implies that there are more than the two to three layers found in all previously measured liquid metals.

Indeed, a theoretical model fit to the measured values of $R(q_z)/R_F(q_z)$ (Fig. 2A, red line) yields the $\rho(z)$ curve shown in Fig. 2B. Although the finer details of this $\rho(z)$ curve may not be unique, two features were independent of the model used: the 2.5-nm-thick layering range (seven to eight well-defined atomic layers) and the Si enrichment of the top layer, indicated by a ρ-value less than that of ρ_{bulk}, which corresponds to ~ 70 atomic % Si. This value agrees well with the 67 atomic % calculated from the Gibbs adsorption rule for an ideal binary solution (*18*).

No variation was found in the measured $R(q_z)$ from $T_e = 359$ °C up to 371 °C. At 371 °C, $R(q_z)/R_F(q_z)$ changed abruptly (Fig. 2A, curve with black squares). By monitoring $R(q_z)$ at a fixed q_z while varying the temperature (Fig. 2B, inset), we found the surface phase transition at 371 °C to be reproducible and to exhibit no hysteresis (<0.1°C). The narrow width of 0.17 °C suggests a first-order phase transition.

The surface-parallel structure was explored by grazing incidence x-ray diffraction (GIXD). X-rays impinging on the liquid AuSi surface well below the critical angle penetrated the surface only evanescently, to a depth of ~ 1.4 nm (*19*), and produced a diffraction pattern for only the top ~ 5 atomic surface layers. The GIXD pattern measured for 359 °C $\leq T \leq$371 °C (Fig. 3) showed sharp diffraction peaks indicative of long-range lateral ordering. A broad peak, characteristic of a liquid, was also observed. The GIXD pattern was indexed in a 2D rectangular lattice of dimensions **a**=7.386 Å and **b**=9.386 Å. A full-pattern refinement yielded the Au_4Si_8 structure shown in the right inset of Fig. 3. The high-T surface phase, which forms at 371 °C and exists up to at least 410 °C, also exhibits a set of sharp GIXD peaks but at different q_{xy}

positions (*20*) than those of the 359 °C $< T <$371 °C surface phase.

The GIXD peak intensities in the low-T phase were not affected by sample rotation around the surface-normal axis, indicating that the diffracting monolayer consists of a fine powder of randomly oriented crystallites. Debye-Scherrer analysis of the line shapes, measured with a high-resolution analyzer crystal, yields a typical crystallite size of $\sim$ 2 to 10 μm. The measured Bragg rods (see the supporting online material) are surface-normal, indicating a quasi-2D crystalline structure. The ~ 1.5 Å^{-1}, width of the rod's q_z intensity distribution implies a crystalline layer thickness of $d = \pi/(1.5\text{Å}^{-1})$, where d is approximately equal to 2 $\mathring{A}$, that is, a monolayer. This result agrees with d value of ≈ 2.5 Å that is estimated from the ratio of the integrated intensities of the GIXD peaks and the broad liquid peak.

Notably, despite the crystalline order, the capillary surface dynamics are still liquid-like; the diffuse scattering measured away from the specular peak exhibits a power-law behavior characteristic of the height-height correlations in liquid surfaces (*21*) (Fig. 3, left inset). The line shape of the diffuse scan (solid line in left inset of Fig. 3) is well reproduced by the capillary wave theory profiles if we use $\gamma_{AuSi} = 780$ mN/m convolved with the experimental resolution function. The compliance with capillary wave theory also indicates that in spite of the larger layering depth, the subsurface ordered layers are laterally liquid, as is the case for all previously measured liquid metals.

The crystalline AuSi monolayer's structure does not resemble those of pure Au, pure Si or any of the reported metastable bulk intermetalics. However, crystalline phases with unit cell dimensions **a**=7.44 Å and **b**=9.33 Å similar to those observed in our study, were reported in thin Au films deposited on a Si(111) surface (*22*). Some of these phases were thought to be surface phases, and some may exist also in the bulk. No reliable thickness of these phases could be obtained by the low-energy electron diffraction and Auger electron spectroscopy techniques that were used. A clear understanding of the formation mechanism, stability, and surface specificity

of the crystalline phases in this system has not yet emerged (*23*). However, the strong Si-Si bonding (*24*) was suggested to play a crucial role, as well as the quasi-2D atomic coordination near the surface (*25*). In our case, the Gibbs adsorption surface enrichment by Si atoms is likely to facilitate the chemical Au-Si bonds that stabilize the crystalline surface layer but which evolve to metallic-like bonding away from the surface (*26*).

The Si packing in the crystalline surface monolayer (Fig. 3, right inset) resembles the covalently bonded, network-forming Si chains suggested to stabilize the amorphous structure of Si-rich AuSi alloys (*15, 16*). A comparison of the unit cell structure presented in Fig. 3 with fig. 1A of Miracle (*15*) indicates that the unit cell packing here is close to the interpenetrating cluster structure recently suggested as the main structural motif of bulk amorphous solids.

The formation of a surface-frozen phase is typically marked by a change in the slope of the surface tension versus temperature curve, $\gamma(T)$, from $d\gamma/dT > 0$ for a crystalline surface to $d\gamma/dT < 0$ for a liquid surface (*3*). Indeed, a positive slope is reported for AuSi above melting (*27*), in line with the crystalline phase reported here. The change to a negative slope, reported to occur at $T \approx 800$ to 900 °C (*27*), should indicate the melting of the ordered surface structure. Similar positive $\gamma(T)$ slopes above melting have been recently reported for AgSn, AgBi, AgIn, InCu, CuSn, MnSn and AuZn binary alloys, implying that the formation of surface-frozen phases may be not an entirely uncommon phenomenon in multi-component liquid alloys.

Beyond its importance for understanding the physics underlying amorphous metallic alloys, AuSi is also of high technological importance, because Au is widely used in interconnecting integrated circuits on Si substrates. AuSi also has important nanoscale applications such as the self-assembly of Si nanowires (*28*) and low-temperature bonding in micro- and nanoelectromechanical devices (*29*). Surface phases are of particular importance for nanotechnology, because properties of objects at the nanometer scale are expected to be dominated by surfaces and interfaces. The discovery of previously unidentified structures bridging the gap between 2D and

3D phases is expected, therefore, to have far-reaching consequences for both fundamental and applied research.

References and Notes

1. J. W. M. Frenken, J. F. Van der Veen, *Phys. Rev. Lett.* **54**, 134 (1985).
2. J. G. Dash, *Phys. Today* **38**, 26 (1985).
3. X. Z. Wu *et al.*, *Science* **261**, 1018 (1993).
4. Z. Dogic, *Phys. Rev. Lett.* **91**, 165701 (2003).
5. A. V. Tkachenko, Y. Rabin, *Phys. Rev. Lett.* **76**, 2527 (1996).
6. B. Yang, D. Gidalevitz, D. Li, Z-q. Huang, S. A. Rice, *Proc. Natl. Acad. Sci. U.S.A.* **96**, 13009 (1999).
7. B. Yang, D. Li, S. A. Rice, *Phys. Rev. B* **67**, 212103 (2003).
8. O. M. Magnussen *et al.*, *Phys. Rev. Lett.* **74**, 4444 (1995)
9. M. J. Regan *et al.*, *Phys. Rev. Lett.* **75**, 2498 (1995).
10. S. E. Donnelly *et al.*, *Science* **296**, 507 (2002).
11. S. H. Oh, Y. Kauffmann, C. Scheu, W. D. Kaplan, and M. Rühle, *Science* **310**, 661 (2005).
12. W. J. Huisman *et al.*, *Nature* **390**, 379 (1997).
13. W. Klement Jr., R. H. Willens, P. Duwez, *Nature* **187**, 869 (1960).
14. J. Weissmüller, *J. Non-Cryst. Solids* **142**, 70 (1992).

15. D. B. Miracle, *Nature Mater.* **3**, 697 (2004).

16. H. W. Sheng *et al.*, *Nature* **439**, 419 (2006).

17. Our unpublished measurements on the liquid eutectic alloys of AuSn and AuGe yielded layering peaks 30 to 50 times lower than that of AuSi.

18. O. G. Shpyrko *et al.*, *Phys. Rev. Lett.* **95**, 106103 (2005).

19. Details of the GIXD experiment are available at Science Online.

20. Because of insufficient reproducibility, the discussion of this pattern must be deferred.

21. S. K. Sinha, E. B. Sirota, S. Garoff, H. B. Stanley, *Phys. Rev. B* **38**, 2297 (1988).

22. A. K. Green, E. Bauer, *J. Appl. Phys.* **47**, 1284 (1976).

23. J. F. Chang *et al.*, *Mat. Chem. Phys.* **83**, 199 (2004).

24. H. S. Chen, D. Turnbull, *J. Appl. Phys.* **38**, 3646 (1967).

25. S. L. Molodtsov, C. Laubschat, G. Kaindl, A. M. Shikin, V. K. Adamchuk, *Phys. Rev. B* **44**, 8850 (1991).

26. V. A. Filonenko, *Russ. J. Phys. Chem.* **43**, 874 (1969).

27. L. Bischoff, J. Teichert, Th. Ganetsos, G. L. R. Mair, *J. Phys. D: Appl. Phys.* **33**, 692 (2000).

28. J. B. Hannon, S. Kodambaka, F. M. Ross, R. M. Tromp, *Nature* **440**, 69 (2006).

29. Y. T. Cheng, L. W. Lin, K. Najafi, *J. Microelectromech. Syst.* **9**, 3 (2000).

30. This work was supported by the U.S. Department of Energy (DOE) grant DE-FG02-88-ER45379 and the U.S.-Israel Binational Science Foundation, Jerusalem. We acknowledge

beamline assistance from J. Gebhardt, T. Graber, and H. Brewer at the Chemistry and Materials Science sector of the Center for Advanced Radiation Sources (ChemMatCARS). ChemMatCARS Sector 15 is principally supported by NSF/DOE grant CHE0087817. The Advanced Photon Source is supported by the U.S. DOE contract W-31-109-Eng-38.

4 April 2006; accepted 25 May 2006

10.1126/science.1128314

Shpyrko, fig1, x21p

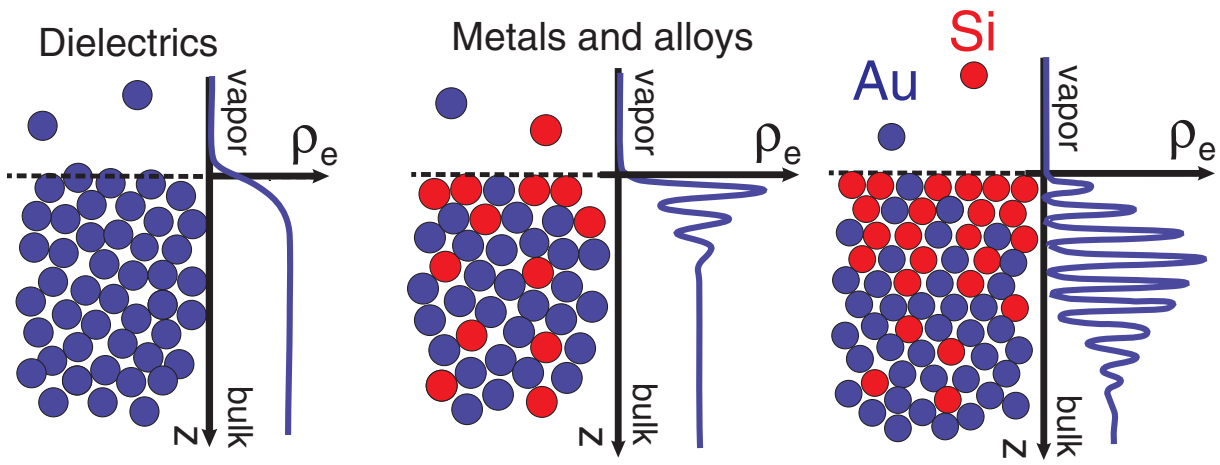

Figure 1: **Fig. 1.** Typical atomic surface structure and corresponding electron density profiles $\rho_e(z)$ of nonlayered dielectric liquids (left), standard layering in liquid metals and alloys (middle) and enhanced layering in AuSi (right).

Shpyrko, fig2, x25p

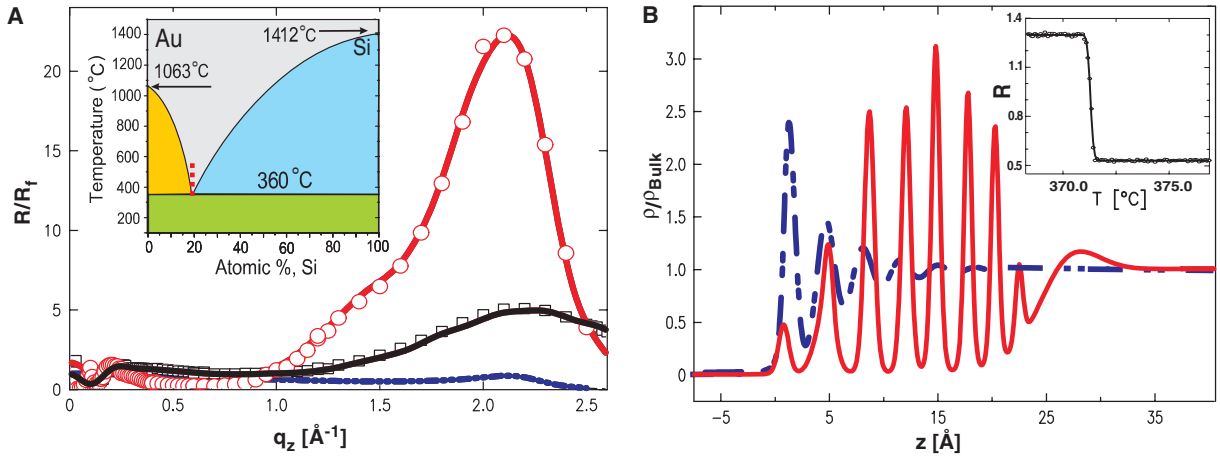

Figure 2: **Fig. 2. (A)** Fresnel-normalized x-ray reflectivity at 370 °C (circles) and 375 °C (squares), the corresponding model fits (red and black lines, respectively), and the curve expected for standard layering (dashed blue line). **(Inset)** Bulk phase diagram of AuSi. Grey area represent a liquid mixture phase, and the blue and yellow areas indicate phase coexistence of solid Si or Au with a liquid alloy. The green area corresponds to phase separated solid Au and solid Si. **(B)** Surface-normal electron density profiles corresponding to the same-line models in (A). **(Inset)** Reflectivity at fixed $q_z = 1.0$ Å^{-1} (circles) versus temperature, with a fit (black line) by an error function centered at 371.29 °C with a width of 0.17 °C.

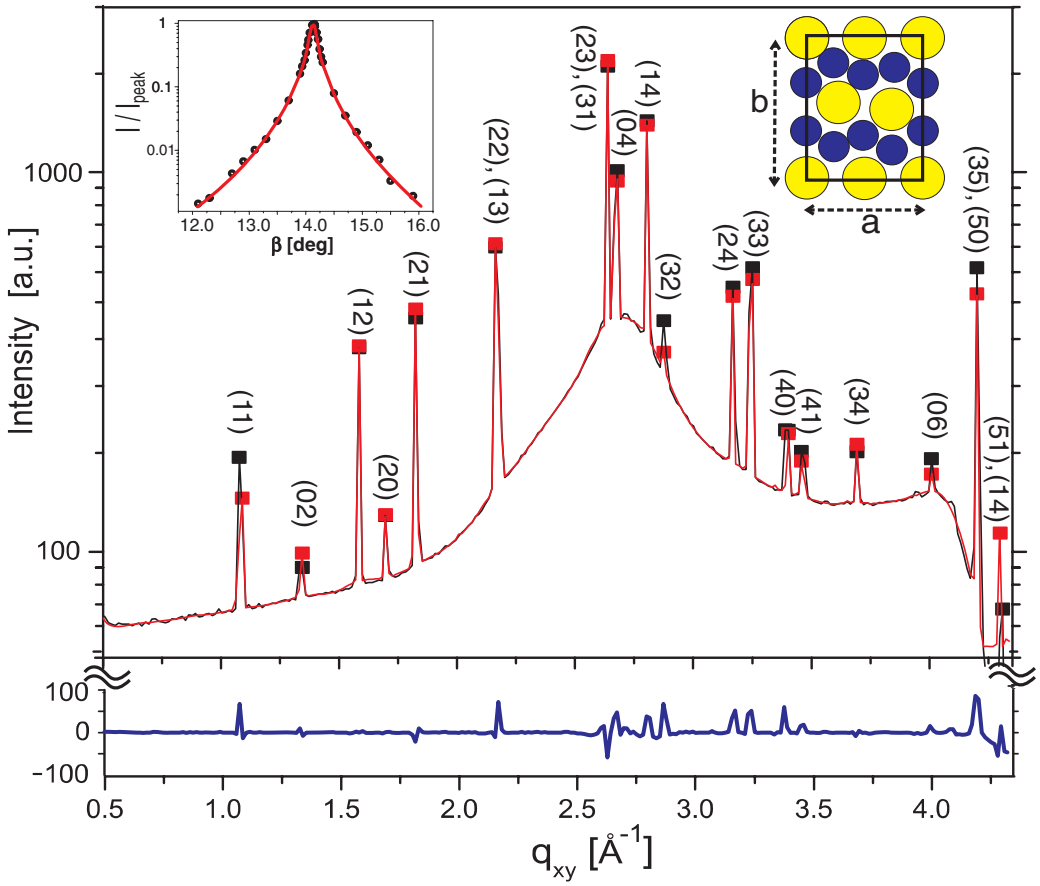

Figure 3: **Fig. 3.** Measured GIXD pattern (black line), theoretical fit (red line), and their difference (blue line) for the $359\ ^{\circ}\mathrm{C} < T < 371\ ^{\circ}\mathrm{C}$ surface phase. a.u., arbitrary unites. (**Left inset)** Diffuse scattering profile versus the output detector angle β for a fixed incidence angle $\alpha = 14.11^{\circ}$ and its fit (line) by the capillary wave theory prediction for $\gamma = 780$ mN/m. I/I_{peak} is the x-ray intensity normalized by the scan's peak intensity value. **(Right inset)** Crystal unit cell obtained from GIXD pattern, where (**a**=7.386 Å, **b**=9.386 Å. Au, yellow circles; Si, blue circles.